Supporting Information

Text S1. Pretreatment of WPCBs.

First of all, WPCBs were subjected to electronic component removal to obtain the substrate boards through thermal desoldering, rolling and falling using an automated dismantling equipment. Subsequently, the substrate boards were crushed into powders using a crusher. The powders were then separated into copper foil powders and non-metal powders via a high-voltage electrostatic sorting device. Finally, the non-metal powders were sieved through a 100-mesh screen to obtain the fine non-metal powders used in experiments.

Table S1 Partial chemical content of NMPs of WPCBs.

Elements	Content (wt%)	Elements	Content (wt%)
Al	4.39	Cr	0.06
B	0.81	Ti	0.12
Ba	0.72	Cu	3.78
Ca	7.46	K	0.07
Fe	0.47	Sr	0.07
Na	0.14	C	26.54
Mg	0.41	Br	6.54
Si	11.55		

Table S2 Components of alkali-free glass fiber powder.

Components	Content (wt%)	Components	Content (wt%)
Al_2O_3	14.52	TiO_2	0.45
SiO_2	53.85	SrO	0.11
Fe_2O_3	0.26	Rb_2O	0.01
CaO	21.1	B_2O_3	6.82
MgO	1.18	CeO_2	0.03
K_2O	0.14	P_2O_5	0.02
Na_2O	0.69	Others	0.82

Table S3 Compositions of pyrolysis oil for N_2-W.

Retention time	Peak area	Percentage	Components
9.555	64760241	53.58	Phenol
11.464	4813471	3.98	Phenol, 2-methyl-
11.779	2332195	1.93	Phenol, 2-bromo-
12.057	3391208	2.81	p-Cresol
12.77	3040374	2.52	Benzofuran, 2,3-dihydro-2-methyl-
13.639	743408	0.61	Phenol, 2-ethyl-
13.904	1187380	0.98	Phenol, 2,4-dimethyl-
14.366	2278545	1.88	Phenol, 4-ethyl-
14.732	534837	0.44	Benzofuran, 2,3-dihydro-2-methyl-
14.984	372790	0.31	Benzofuran, 2,3-dihydro-2-methyl-
15.279	299362	0.25	1,5-Dihydroxy-1,2,3,4-tetrahydronaphthalene
15.46	984569	0.81	2-Propanone, 1-phenoxy-
15.611	231093	0.19	3-Buten-2-one, 4-phenyl-
15.675	363484	0.3	Phenol, 4-propyl-
15.815	27169085	22.48	p-Cumenol
17.394	642741	0.53	Thymol
17.904	318400	0.26	Phenol, 4-(1-methylpropyl)-
18.252	3022370	2.5	2-bromo-4-isopropylphenol
18.882	820492	0.68	Benzene, 1-(1,1-dimethylethyl)-3-ethyl-5-methyl-
19.162	1727205	1.43	1H-Inden-1-one, 2,3-dihydro-3,4,7-trimethyl-
19.292	612963	0.51	Phenol, 2,6-dibromo-
21.303	352385	0.29	3-Buten-2-one, 4-(2,6,6-trimethyl-1-cyclohexen-1-yl)-
24.393	529841	0.44	5-Methyl-2,4-diisopropylphenol
24.549	352183	0.29	2,6-dibromo-4-isopropylphenol

Table S4 Compositions of pyrolysis oil for CO_2-W.

Retention time	Peak area	Percentage	Components
9.557	60510381	55.95	Phenol
11.46	4046619	3.74	Phenol, 2-methyl-
11.776	2036187	1.88	Phenol, 2-bromo-
12.052	2864051	2.65	p-Cresol
12.769	2841250	2.63	Benzofuran, 2,3-dihydro-2-methyl-
13.636	557949	0.52	Phenol, 2-ethyl-
13.9	1023319	0.95	Phenol, 2,4-dimethyl-
14.362	1897744	1.76	Phenol, 4-ethyl-
14.727	417471	0.39	Benzofuran, 2,3-dihydro-2-methyl-
14.979	287889	0.27	Benzofuran, 2,3-dihydro-2-methyl-
15.276	269228	0.25	1,5-Dihydroxy-1,2,3,4-tetrahydronaphthalene
15.456	581692	0.54	2-Propanone, 1-phenoxy-
15.608	241704	0.22	3-Buten-2-one, 4-phenyl-
15.671	308063	0.28	Phenol, 4-propyl-
15.807	23405591	21.65	p-Cumenol
17.393	494370	0.46	Thymol
17.902	245065	0.23	Phenol, 4-(1-methylpropyl)-
18.247	2445061	2.26	2-bromo-4-isopropylphenol
18.878	603218	0.56	Benzene, 1-(1,1-dimethylethyl)-3-ethyl-5-methyl-
19.159	1416961	1.31	1H-Inden-1-one, 2,3-dihydro-3,4,7-trimethyl-
19.297	481192	0.45	Phenol, 2,6-dibromo-
21.302	247923	0.23	trans-.beta.-Ionone
21.403	210481	0.19	1,1,4,5,6-Pentamethyl-2,3-dihydro-1H-indene
24.394	376404	0.35	5-Methyl-2,4-diisopropylphenol

Table S5 Compositions of pyrolysis oil for N_2-W-G.

Retention time	Peak area	Percentage	Components
9.581	65081006	51.55	Phenol
11.468	3742442	2.96	Phenol, 2-methyl-
11.783	1966879	1.56	Phenol, 2-bromo-
12.059	2791537	2.21	p-Cresol
12.764	2450934	1.94	Benzofuran, 2,3-dihydro-2-methyl-
13.642	582412	0.46	Phenol, 2-ethyl-
13.904	1058581	0.84	Phenol, 2,4-dimethyl-
14.365	1965960	1.56	Phenol, 4-ethyl-
14.728	415929	0.33	2H-1-Benzopyran, 3,4-dihydro-
15.466	599516	0.47	2-Propanone, 1-phenoxy-
15.674	336642	0.27	Phenol, 4-propyl-
15.815	26750255	21.19	p-Cumenol
16.627	250605	0.2	Phenol, 4-propyl-
17.392	539563	0.43	Thymol
17.899	298806	0.24	Phenol, 4-(1-methylpropyl)-
18.247	2820850	2.23	2-bromo-4-isopropylphenol
18.879	839116	0.66	Benzene, 1-(1,1-dimethylethyl)-3-ethyl-5-methyl-
19.157	1724768	1.37	1H-Inden-1-one, 2,3-dihydro-3,4,7-trimethyl-
19.283	536790	0.43	Phenol, 2,6-dibromo-
24.373	607974	0.48	5-Methyl-2,4-diisopropylphenol
24.541	268451	0.21	2,6-dibromo-4-isopropylphenol
26.268	871734	0.69	p-Hydroxybiphenyl
32.211	481173	0.38	Androst-1-ene-3,17-dione, (5.alpha.)-
34.465	4488722	3.56	Bisphenol A
35.204	298463	0.24	2-(4'-Hydroxyphenyl)-2-(4'-methoxyphenyl)propane
35.993	703915	0.56	Prosulfocarb
36.344	2533848	2.01	Monobromobisphenol A
36.853	405569	0.32	1H-Inden-5-ol, 2,3-dihydro-3-(4-hydroxyphenyl)-1,1,3-trimethyl-
37.9	321399	0.25	Dibromobisphenol A
39.303	264968	0.21	2-bromo-4-(2-(4-(2-hydroxypropoxy)phenyl)propan-2-yl)phenol
39.405	240594	0.19	trans-.beta.-Ionone

Table S6 Compositions of pyrolysis oil for N_2-W-Cu.

Retention time	Peak area	Percentage	Components
5.865	3466006	3.22	2-Pentanone, 4-hydroxy-4-methyl-
9.563	60002545	55.78	Phenol
11.474	3913523	3.64	Phenol, 2-methyl-
11.795	871684	0.81	Phenol, 2-bromo-
12.065	3125923	2.91	p-Cresol
12.772	2809065	2.61	Benzofuran, 2,3-dihydro-2-methyl-
13.645	702287	0.65	Phenol, 2-ethyl-
13.911	963072	0.9	Phenol, 2,3-dimethyl-
14.37	2021383	1.88	Phenol, 4-ethyl-
14.732	485009	0.45	2H-1-Benzopyran, 3,4-dihydro-
14.98	407783	0.38	Benzofuran, 2,3-dihydro-2-methyl-
15.287	330112	0.31	1H-Indene-1,2-diol, 2,3-dihydro-1-methyl-, cis-
15.455	1019048	0.95	2-Propanone, 1-phenoxy-
15.611	208264	0.19	1-Methylindan-2-one
15.809	22516227	20.93	p-Cumenol
17.407	528308	0.49	3-Methyl-4-isopropylphenol
17.912	206664	0.19	Phenol, 2-(1-methylpropyl)-
18.262	969718	0.9	2-bromo-4-isopropylphenol
18.881	698397	0.65	Benzene, 1-(1,1-dimethylethyl)-3-ethyl-5-methyl-
19.166	1358894	1.26	5',6',7',8'-Tetrahydro-2'-acetonaphthone
19.368	210648	0.2	Biphenyl
21.309	273495	0.25	2,6-Diisopropylanisole
21.408	194703	0.18	1H-Inden-1-one, 2,3-dihydro-3,3,5,7-tetramethyl-
24.449	293947	0.27	5-Methyl-2,4-diisopropylphenol

Table S7 The common mechanism functions used for solid-phase reactions.

Number	Model	f(α)
1	Šesták-Berggren model (Šesták *et al.,* 1971)	$(1-\alpha)^n\alpha^m[-\ln(1-\alpha)]^p$
2	Jander 3-D diffusion (Wang *et al.,* 2023)	$\frac{3}{2}(1-\alpha)^{\frac{2}{3}}\left[1-(1-\alpha)^{\frac{1}{3}}\right]^{-1}$
3	Ginstling-Brounshtein 3-D diffusion (Wang *et al.,* 2023)	$\frac{3}{2}\left[(1-\alpha)^{-\frac{1}{3}}-1\right]^{-1}$
4	Anti-Jander 3-D (Yao *et al.,* 2018)	$\frac{3}{2}(1+\alpha)^{\frac{2}{3}}\left[(1+\alpha)^{\frac{1}{3}}-1\right]^{-1}$
5	Z-L-T 3-D (Yao *et al.,* 2018)	$\frac{3}{2}(1-\alpha)^{\frac{4}{3}}\left[(1-\alpha)^{-\frac{1}{3}}-1\right]^{-1}$

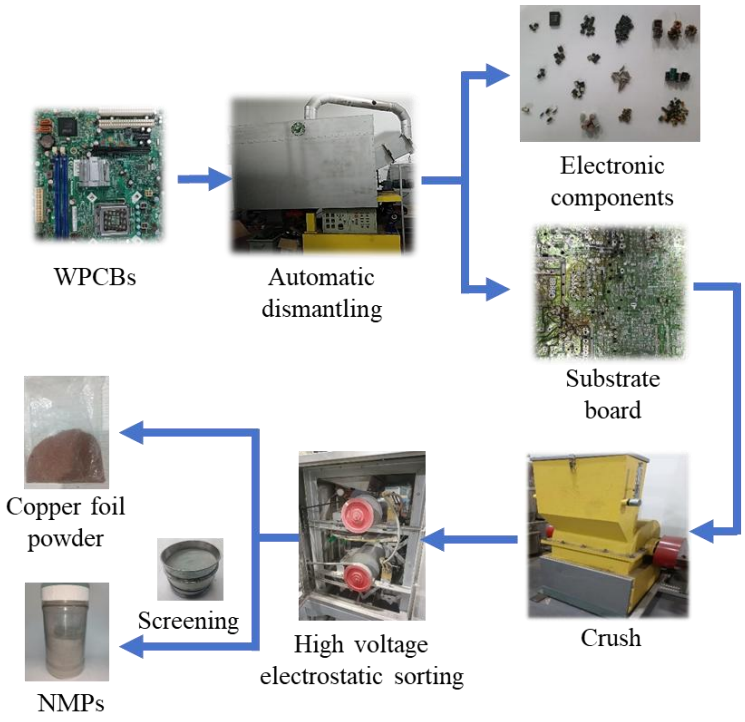

Fig. S1 Dismantling, crushing, and sorting of waste printed circuit boards to obtain non-metal powders for experiment.

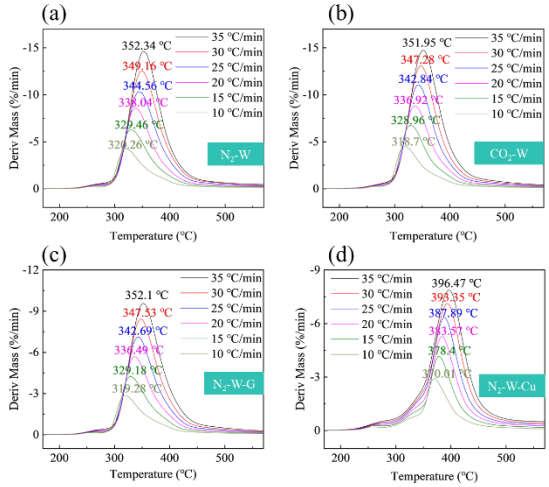

Fig. S2 DTG analysis of (a) NMPs of WPCBs in N_2, (b) NMPs of WPCBs in CO_2, (c) NMPs of WPCBs with fiber glass in N_2 and (d) NMPs of WPCBs with Cu in N_2.

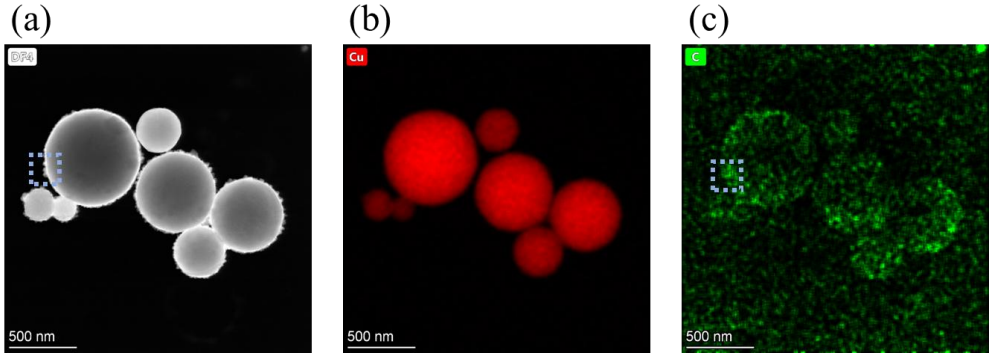

Fig. S3 Transmission electron microscopy (TEM) images and Energy Dispersive Spectroscopy (EDS) mapping images of the copper particles after debromination reaction (a) TEM image, (b) EDS mapping image of Cu element, (c) EDS mapping image of C element.

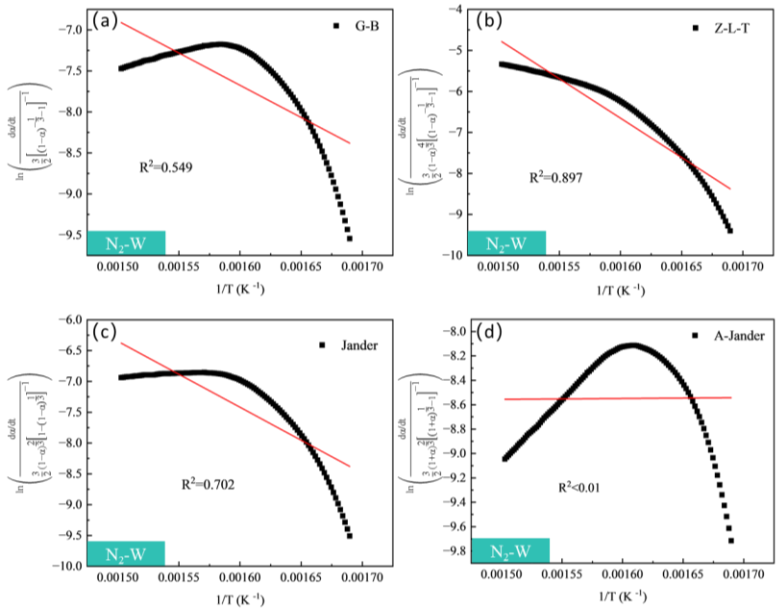

Fig. S4 The liner fitting results of some commonly used reaction mechanism functions for N_2-W (a) Ginstling-Brounshtein 3-D Diffusion model (G-B), (b) Zhuralev-Lesokin-Tempelman 3-D model (Z-L-T), (c) Jander 3-D diffusion model (Jander) and (d) Anti-Jander 3-D model (A-Jander).

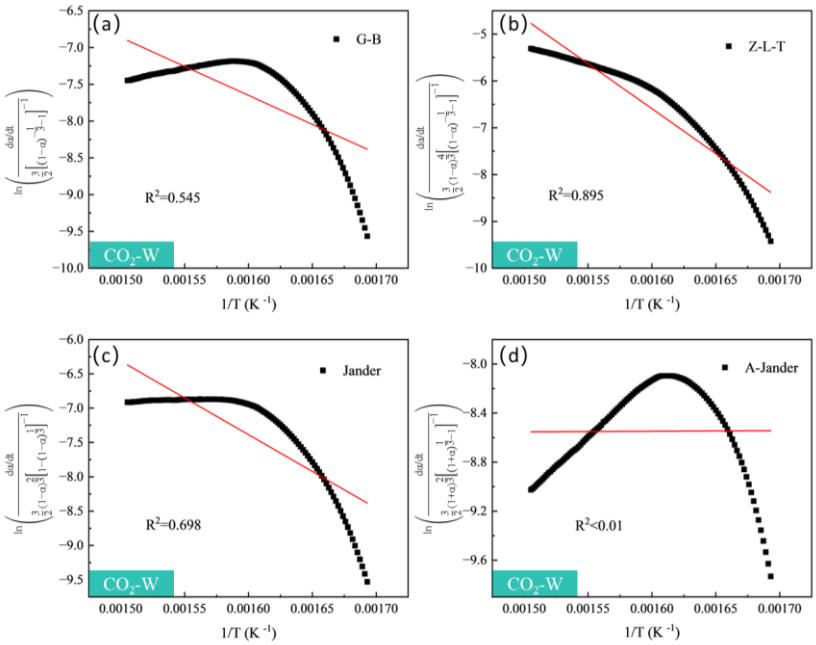

Fig. S5 The liner fitting results of some commonly used reaction mechanism functions for CO_2-W (a) Ginstling-Brounshtein 3-D Diffusion model (G-B), (b) Zhuralev-Lesokin-Tempelman 3-D model (Z-L-T), (c) Jander 3-D diffusion model (Jander) and (d) Anti-Jander 3-D model (A-Jander).

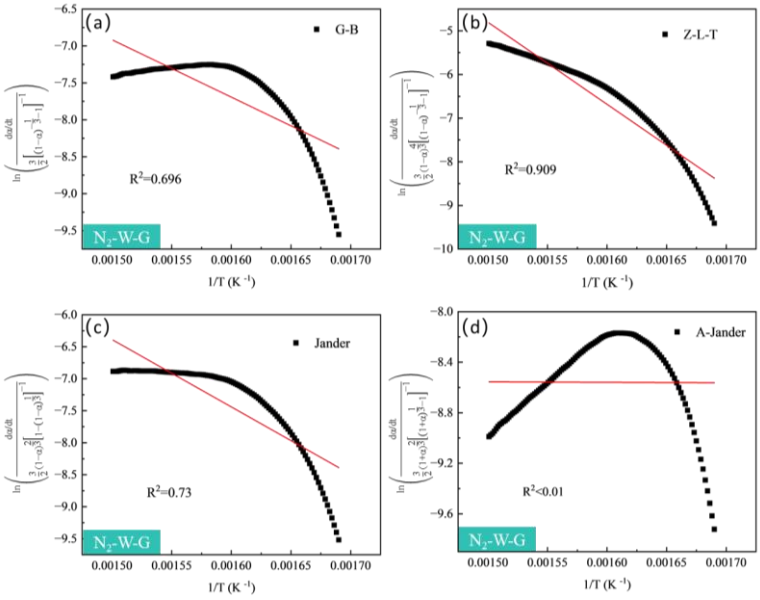

Fig. S6 The liner fitting results of some commonly used reaction mechanism functions for N_2-W-G (a) Ginstling-Brounshtein 3-D Diffusion model (G-B), (b) Zhuralev-Lesokin-Tempelman 3-D model (Z-L-T), (c) Jander 3-D diffusion model (Jander) and (d) Anti-Jander 3-D model (A-Jander).

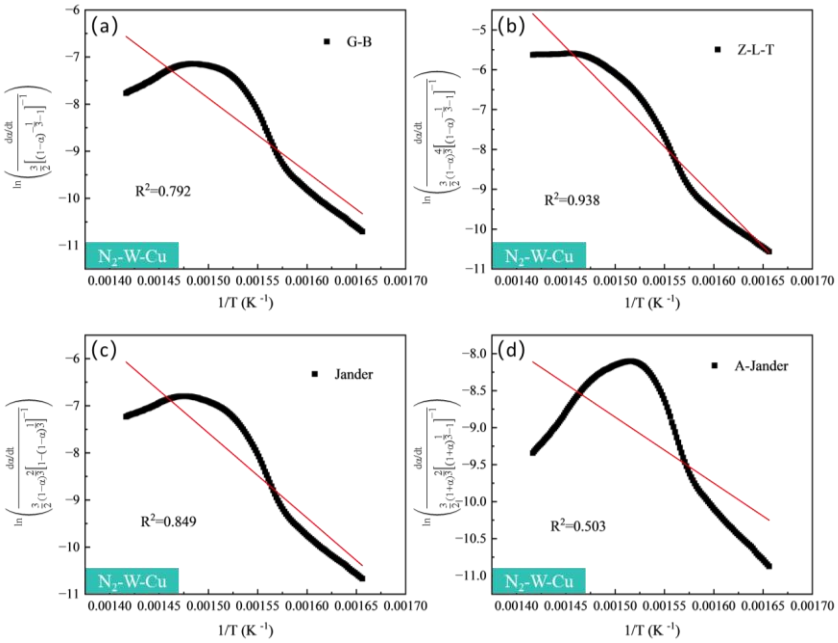

Fig. S7 The liner fitting results of some commonly used reaction mechanism functions for N_2-W-Cu (a) Ginstling-Brounshtein 3-D Diffusion model (G-B), (b) Zhuralev-Lesokin-Tempelman 3-D model (Z-L-T), (c) Jander 3-D diffusion model (Jander) and (d) Anti-Jander 3-D model (A-Jander).

References for supporting information

Šesták, J.; Berggren, G. Study of the kinetics of the mechanism of solid-state reactions at increasing temperatures. Thermochim. Acta. 1971, 3(1), 1-12.

Wang, Y.; Yu, G.; Xie, S.; Jiang, R.; Li, C.; Xing, Z. Pyrolysis of food waste digestate residues for biochar: Pyrolytic properties, biochar characterization, and heavy metal behaviours. Fuel (Guildford). 2023, 353, 129185.

Yao, X.; Yu, Q.; Han, Z.; Xie, H.; Duan, W.; Qin, Q. Kinetic and experimental characterizations of biomass pyrolysis in granulated blast furnace slag. Int. J. Hydrogen Energ. 2018, 43(19), 9246-9253.